Article | Received 7 June, 2026; Accepted 14 September, 2026; Published 10 October, 2026
https://doi.org/10.55092/pe20260020

Study on the influence of freeze-thaw cycles on the pore structure and mechanical properties of magnetic slurry

Anlong Hu[1], Yongsheng Ju[1], Yong Wei[1], Zhipeng Shang[1], Jie Liu[2]and Xinlong Yao[2,*]

[1] Economic and technological research institute, State grid Gansu Electric Power Company, Lanzhou, China

[2] College of Civil Engineering and Architecture, China Three Gorges University, Yichang, China

* Correspondence author; E-mail: 18297488699@163.com.

Abstract: This study investigates the structural damage evolution and mechanical degradation of epoxy-modified magnetic cementitious slurry under freeze-thaw cycles. To elucidate the damage mechanism, slurries with varying magnetic powder contents were subjected to freeze-thaw testing. The evolution of pore distribution was quantitatively analyzed using Computed Tomography (CT) and Scanning Electron Microscopy (SEM) via image binarization. The results reveal that: (1) An increase in magnetic powder content significantly mitigated structural damage, indicating that magnetic particles positively contribute to the freeze-thaw resistance of the slurry; (2) The application of an external magnetic field significantly enhanced frost resistance, with magnetically aligned specimens exhibiting reduced damage levels post-cycling compared to non-magnetized controls; (3) Under identical magnetic powder contents, specimens subjected to a magnetic field demonstrated notably higher compressive strength and a significantly lower strength loss rate after freeze-thaw cycles compared to those without magnetic field treatment; (4) As the magnetic powder content increased, the porosity within the specimens gradually decreased, resulting in a more compact structure and improved freeze-thaw resistance; (5) Magnetic particles self-assembled into four primary chain morphologies: through, branched, isolated, and bundled chains. The evolution of these morphologies plays a critical role in governing the mechanical properties and structural stability of the composite.

Keywords: freeze-thaw cycles; pore structure; magnetic slurry; failure morphology

1. Research background

In northern China, freeze-thaw damage is widespread and highly destructive. Many concrete structures located in cold climatic zones face severe challenges from freeze-thaw cycles [1,2]. This issue is particularly prominent in high-altitude areas. Due to the extremely harsh climatic conditions, major construction projects such as the Sichuan-Tibet Railway must withstand the significant test of freeze-thaw damage during both construction and operation phases. In high-latitude cold regions like Northeast China, key structures such as dams and bridges, which are subjected to repeated freeze-thaw damage over the long term, often develop serious defects including concrete cracking and steel bar exposure. These problems not only impair the normal functional performance of the structures but also pose a major threat

Copyright©2026 by the authors. Published by ELSP. This work is licensed under Creative Commons Attribution 4.0 International License, which permits unrestricted use, distribution, and reproduction in any medium provided the original work is properly cited.

to their service life. In the coastal areas of North China, concrete structures such as port terminals in the marine environment not only endure frequent wet-dry cycles caused by seawater but also undergo repeated freeze-thaw cycle impacts in winter. Such complex environmental conditions can generate frost heave pressure inside the concrete [3–6], thereby reducing the service life of the concrete structures.

It is evident that long-term freeze-thaw cycles can cause severe damage to concrete structures, such as a significant decrease in strength, reduced impermeability, and large-scale spalling of the concrete surface. More seriously, the numerous microcracks generated by freeze-thaw cycles can act as channels for water transport within the concrete. The presence of these microcracks accelerates the freeze-thaw deterioration process of concrete structures and shortens the service life of concrete structures operating in freeze-thaw environments [7].

An in-depth study of the mechanism of freeze-thaw damage reveals that its root cause lies in the complex reactions of pore solutions—saturated or nearly saturated—inside the material during alternating positive and negative temperature changes. The capillary effects and drastic changes in pore pressure caused by this repeated process lead to irreversible changes in the microstructure and composition of the material, ultimately resulting in macroscopic damage such as crack propagation and surface spalling [8–10]. Moreover, the hardened cement paste formed by the hydration of cement mixed with water has a wide range of internal pore sizes, ranging from the nanoscale to the millimeter scale [7].

To improve and enhance the performance of structures themselves under freeze-thaw cycles and strengthen their freeze-thaw resistance, efforts must be made simultaneously in two key technical aspects: on one hand, enhancing the internal bonding capacity and bond strength of the structural material itself; on the other hand, adopting effective measures to increase the internal density of the structural material and reduce the presence of pores. Based on this basic concept and technical requirement, this paper focuses on the changes and development patterns of the mechanical properties of epoxy resin magnetically self-aggregating cement grout under freeze-thaw cycles [11]. Epoxy resin magnetically self-aggregating cement grout is a new type of composite material, composed of multiple materials including epoxy resin, curing agent, magnetic powder, Portland cement, and sulphoaluminate cement. Among these components, the magnetic powder used in the epoxy resin magnetically self-aggregating cement grout has a micron-level particle size. During the hydration and hardening process of the cement grout, it can effectively fill a part of the pore space, playing an excellent pore-filling role. Furthermore, under the control of an external magnetic field, the movement and distribution of the magnetic powder can be regulated, thereby achieving better filling of pores in the structure. Meanwhile, the addition of epoxy resin and curing agent significantly improves the bonding capacity and integrity between the various components of the structural material, as well as enhances the material's mechanical properties [12-16].

This study aims to investigate the mechanism by which magnetic powder content ratio and external magnetic field conditions affect the frost resistance of epoxy resin magnetically self-aggregating cement grout. By controlling different magnetic powder mixing ratios and combining the application of external magnetic fields with varying intensities, the regulatory effects of these factors on the internal pore structure of the material and the intrinsic relationship between such effects and frost resistance are analyzed. Through the testing of the material's compressive performance, the damage evolution process of cement-based materials under freeze-thaw cycles is comprehensively understood and mastered. A detailed study and analysis are conducted on the mechanical properties of epoxy resin magnetically

self-aggregating cement grout after freeze-thaw cycles, so as to accurately describe the damage development law and performance evolution characteristics of cement-based composites in freeze-thaw environments. Distinct from traditional studies on the freeze-thaw resistance of cement-based composites, this paper achieves a significant breakthrough in microstructure regulation and durability enhancement by introducing magnetic slurry. Through the squeezing effect of magnetic chains, the magnetic slurry forces the deformation and expulsion of entrapped air bubbles, thereby compressing pore volume, blocking capillary channels, and significantly reducing porosity.

This technique holds particular applicability for the micro-crack grouting repair of concrete structures in frigid environments. The research results can provide important technical support for the application of this material in civil engineering structures in frigid regions, especially in engineering components that need to withstand repeated freeze-thaw cycles (such as bridges, dams, and hydraulic structures). Meanwhile, the results also offer practical references for the development and optimization of new functional building materials, and hold significant practical significance and guiding value for the promotion and practical engineering application of this material.

2. Freeze-thaw cycle test

2.1. Preparation of specimens

To conduct an in-depth study on the effect of freeze-thaw cycles on the mechanical properties of magnetic slurries, this paper designs and prepares 6 types of new epoxy resin magnetic cement slurries with different magnetic powder ratios. The selection of raw materials and mix proportions of these slurries are all carefully designed to ensure the scientific validity and reliability of the test results.

The water-cement ratio of the slurry is controlled at 0.4. The cement used adopts a composite formula of Portland cement and sulphoaluminate cement, with the two mixed in a ratio of 4:1. The dosage of water-based epoxy resin is controlled at 6% of the cement content, and the dosage of curing agent is 5.1% of the cement content. To improve the rheological properties and stability of the slurry, a flocculant and a water reducer are also added respectively, with their dosages being 5% and 0.8% of the cement content.

As the core material in this study, the dosage of magnetic powder is the key variable parameter. The test designs 6 different magnetic powder dosage gradients: 0%, 5%, 10%, 15%, 20%, and 25%. The detailed material mix proportions and dosage parameters of the cement slurries in each group are shown in Table 1.

Table 1. Mix ratio of new-type epoxy resin magnetic slurry.

Number	Cement	Water-cement ratio	Epoxy resin	Curing agent	Magnetic powder
1	PO:SAC=4:1	0.4	6%	5.1%	0%
2	PO:SAC=4:1	0.4	6%	5.1%	5%
3	PO:SAC=4:1	0.4	6%	5.1%	10%
4	PO:SAC=4:1	0.4	6%	5.1%	15%
5	PO:SAC=4:1	0.4	6%	5.1%	20%
6	PO:SAC=4:1	0.4	6%	5.1%	25%

Based on epoxy resin magnetic cement slurries with 6 different magnetic powder contents, two specifications of cubic specimens were prepared respectively in accordance with the test requirements.

Among them, the small-sized specimens with a side length of 2 cm were mainly used for compressive strength testing, while the large-sized specimens with a side length of 4 cm were specifically used for mass loss measurement. During the preparation process, two groups of samples were made for the slurry of each mix ratio: the first group was cured naturally without any external magnetic field applied; the second group was treated with an external magnetic field (as shown in Figure 1) to modify the pores in the slurry. To minimize experimental error and ensure data reliability, three replicate specimens were tested for each group. The final result was taken as the arithmetic mean of the three measurements. The number of specimens produced for each group was strictly determined in line with the test statistical requirements, with a total of 6 specimens manufactured. Among these, 3 specimens were used to determine the reference compressive strength value before freeze-thaw cycles (denoted as e_0) in accordance with the provisions of the GB/T 17671 standard, and the other 3 specimens were specifically used for the freeze-thaw cycle test.

To ensure uniform dispersion of the magnetic particles, the slurry was thoroughly stirred during preparation. Subsequently, the mixture was cast into molds and subjected to a vertically upward gradient magnetic field of 5000 Gs. This magnetic field was maintained until the slurry solidified to lock the formed magnetic chain structure. Upon hardening, the magnetic field was removed. All specimens were demolded 24 hours after casting to prevent quality issues caused by premature or delayed demolding. Immediately after demolding, the specimens were cured under strictly controlled conditions (20 ± 2 °C, 95% relative humidity) until the specified testing age of 28 days. This standardized curing system ensures that all specimens are tested under the same environmental conditions, providing a guarantee for the accuracy of the results.

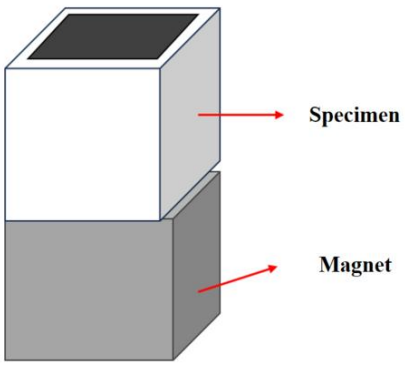


Figure 1. Schematic diagram of applied magnetic field on sample.

2.2. Freeze-thaw cycle test method

Before conducting the freeze-thaw test, all test specimens to be tested must undergo strict preprocessing and initial state recording. First, use a clean rag or absorbent paper to carefully wipe off the attached moisture on the surface of the specimens to ensure the surface is dry and clean. Then, accurately weigh the mass of each specimen and record the data in detail. At the same time, a comprehensive inspection of the specimens' appearance should be carried out to record whether there are initial cracks, holes, or other defects on the specimen surfaces, providing a reference for the subsequent analysis of test results.

During the test, place the preprocessed specimens in the specimen boxes, ensuring the specimens are stably positioned inside the boxes to avoid movement or collision during the test. Subsequently,

slowly pour drinking water into the specimen boxes until the water level is 3-5 mm above the top surface of the specimens, ensuring the specimens can fully come into contact with water throughout the test. After filling with water, move the specimen boxes containing the specimens into the freezing chamber to start the freeze-thaw cycle test.

The entire freeze-thaw cycle process is strictly controlled according to the specified time. Each freeze-thaw cycle lasts for 3 hours, with the freezing phase and thawing phase each taking 1.5 hours. During the freezing phase, the temperature inside the freezing chamber is always maintained at a constant low temperature of -20°C, ensuring the water inside the specimens is fully frozen to generate expansion stress. When the freezing time is reached, take the specimens out of the freezing chamber and transfer them to an environment with a temperature of 20°C for thawing. In accordance with the test design requirements, conduct freeze-thaw tests with different cycle times (e.g., 25 cycles, 50 cycles, 100 cycles). After the completion of each stage, inspect and record the state of the specimens.

2.3. CT test

After the completion of the freeze-thaw cycle test, to conduct an in-depth analysis of the changes in the specimens, it is necessary to perform CT scan detection on the specimens post-test. The acquired CT cross-sectional images then require professional image processing and analysis. The specific image processing process is accomplished using ImageJ, a professional image analysis software.

First, import the obtained CT cross-sectional images into the ImageJ software. Subsequently, utilize the built-in image processing functions of the software to perform binarization processing on the original images. The purpose of binarization processing is to convert each pixel in the image into two colors—black and white—so that the pore regions and the solid material regions form a sharp contrast, facilitating subsequent quantitative analysis.

After completing the binarization processing, use the processed images to calculate the porosity on the cross-section. To ensure the objectivity and reproducibility of the pore structure analysis, the binarization segmentation of CT and SEM images was performed using Otsu's method (Maximum Between-Class Variance Method) in the ImageJ software. This algorithm automatically calculates the optimal threshold by maximizing the separability between the pore phase (dark pixels) and the solid matrix phase (bright pixels), thereby minimizing human intervention errors. This value is a crucial indicator for evaluating the compactness of the material and the degree of freeze-thaw damage, providing key data support for subsequent performance evaluation and mechanism analysis. The entire analysis process must be carried out in strict accordance with standard operating procedures to ensure the accuracy and reliability of the data.

3. Freeze-thaw cycle test

3.1. Failure mode

Figures 2, 3, and 4 show the appearance of specimens with different magnetic powder contents after 25, 50, and 100 freeze-thaw cycles under the condition of no magnetic field. It can be seen from these images that after 25 freeze-thaw cycles, all specimens showed no signs of damage, with smooth surfaces and no cracks or spalling. After 50 freeze-thaw cycles, slight spalling appeared on the surface of each specimen, but the cracks were not obvious and no irreversible damage occurred. After 100 freeze-thaw cycles, all

specimens suffered varying degrees of damage, with obvious and penetrating surface cracks accompanied by spalling.

Figures 5, 6, and 7, on the other hand, display the appearance changes of specimens with the same magnetic powder content after 25, 50, and 100 freeze-thaw cycles under the action of a magnetic field. Under the magnetic field condition, after 25 freeze-thaw cycles, only a few small cracks appeared on the surface of the specimens, and no spalling was observed. After 50 freeze-thaw cycles, slight spalling occurred on the surface of the specimens, but no irreversible damage was caused, and the cracks began to become obvious. After 100 freeze-thaw cycles, the specimens generally showed damage, with significant surface cracks accompanied by spalling.

By comparing the results of the above two groups of experiments, it can be found that the damage to the specimens under the condition of no magnetic field is more serious. This indicates that the application of a magnetic field can significantly improve the frost resistance of epoxy resin magnetic slurry and reduce the structural damage caused by freeze-thaw cycles.

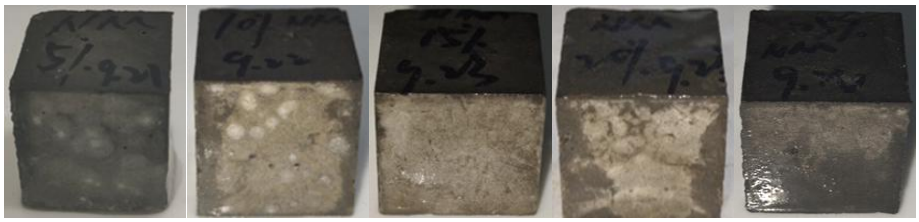


Figure 2. Appearance and morphology of the specimen without magnetic field applied after 25 freeze-thaw cycles.

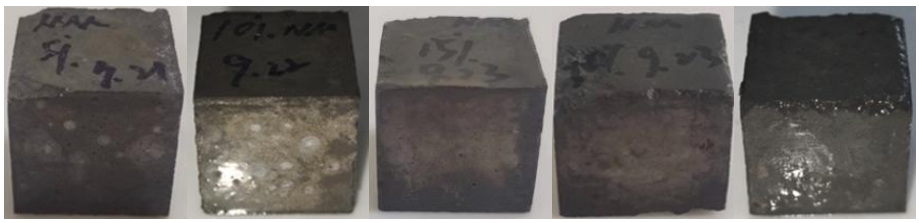


Figure 3. Appearance and morphology of the specimen without magnetic field applied after 50 freeze-thaw cycles.

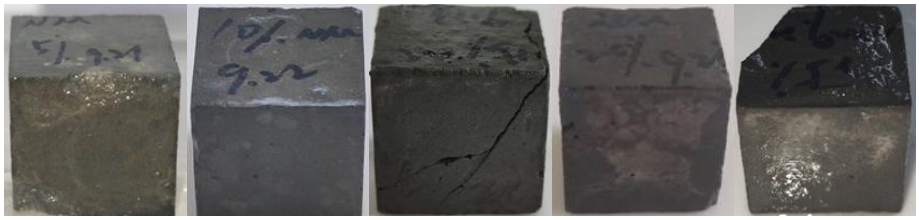


Figure 4. Appearance and morphology of the specimen without magnetic field applied after 100 freeze-thaw cycles.

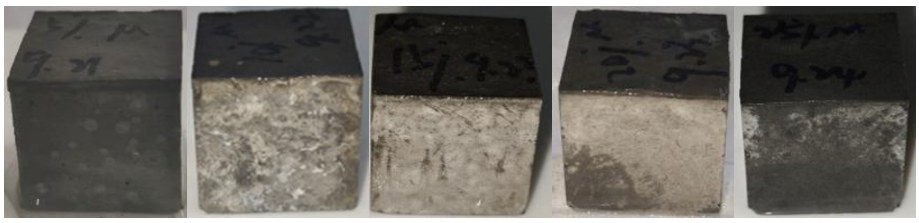


Figure 5. Appearance and morphology of the specimen with magnetic field applied after 25 freeze-thaw cycles.



Figure 6. Appearance and morphology of the specimen with magnetic field applied after 50 freeze-thaw cycles.



Figure 7. Appearance and morphology of the specimen with magnetic field applied after 100 freeze-thaw cycles.

3.2. Compressive performance

The compressive strength of the specimens was tested before and after the freeze-thaw cycle test, and the results are shown in Figure 8. Before the test, the compressive strength of the specimens without a magnetic field applied was lower than that of the specimens with a magnetic field applied, and the compressive strength of both increased with the increase in magnetic powder content. When the magnetic powder content was 15%, the compressive strength reached the maximum value; when the magnetic powder content exceeded 15%, the compressive strength decreased sharply. After the test, the compressive strength of both the specimens without and with a magnetic field applied decreased. However, when the magnetic powder content was less than 15%, the compressive strength increased with the increase in magnetic powder content; when the magnetic powder content exceeded 15%, the compressive strength decreased with the increase in magnetic powder content. In addition, the difference in compressive strength between the specimens without and with a magnetic field applied increased significantly after the test.

By further observing the compressive strength loss rate of the specimens after freeze-thaw cycles, it was found that the compressive strength loss rate of the specimens without a magnetic field applied was significantly higher than that of the specimens with a magnetic field applied. Among the specimens without a magnetic field applied, the maximum compressive strength loss rate was 9.76% and the minimum was 5.65%. The maximum loss rate occurred in the specimen with a 15% magnetic powder content, and the minimum loss rate occurred in the specimen with a 25% magnetic powder content. Among the specimens with a magnetic field applied, the maximum compressive strength loss rate was 6.06% and the minimum was 2.40%. Moreover, with the increase in magnetic powder content, the compressive strength loss rate of the specimens gradually decreased. It is particularly noteworthy that the minimum compressive strength loss rates of both the specimens without and with a magnetic field

applied appeared in the specimens with a 25% magnetic powder content. This indicates that the increase in magnetic powder content not only improves the compressive strength of the specimens but also enhances their ability to resist the effect of freeze-thaw cycles.

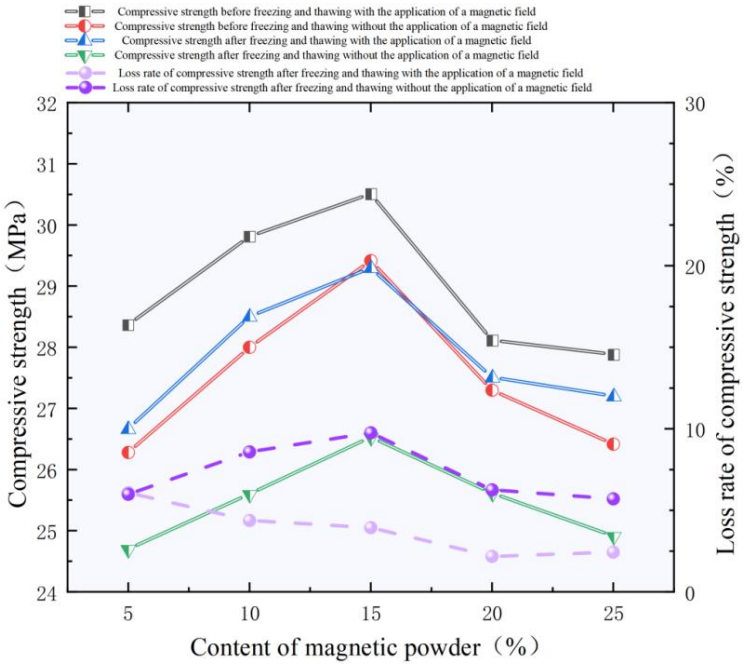
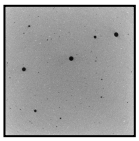
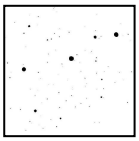
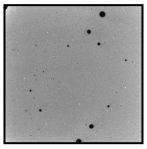
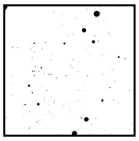
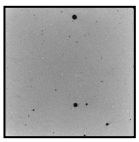
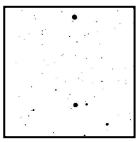
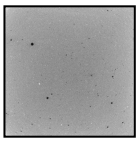
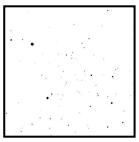
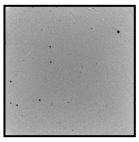
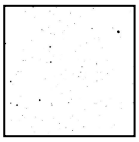
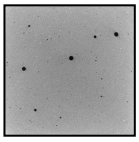
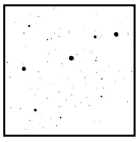
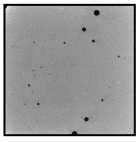
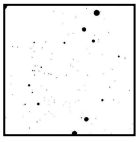
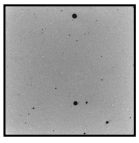
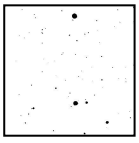
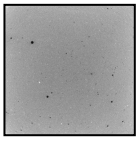
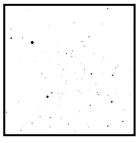
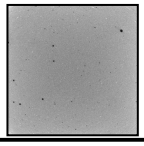
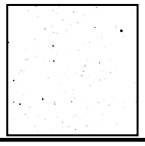


Figure 8. Compressive strength and strength loss of specimens after freeze-thaw cycles.

3.3. Porosity inside the specimen structure

Table 2 shows the CT slices and their binarized images of the specimens under the conditions of no magnetic field applied and magnetic field applied. Figure 9 further compares the porosity of the internal structure of the specimens under different magnetic powder contents. Under the condition of no magnetic field applied, with the increase of magnetic powder content, the porosity in the specimens gradually decreases. When the magnetic powder content is the lowest, the porosity of the specimen is the highest, reaching 2.46%; when the magnetic powder content increases to the highest, the porosity drops to the lowest, which is 1.43%. Under the condition of applying a magnetic field, the variation trend of the porosity of the specimens is similar, but there are also some significant differences. With the increase of magnetic powder content, the porosity also shows a downward trend. The maximum porosity is 2.43%, which occurs when the magnetic powder content is low; the minimum porosity is 1.32%, which occurs when the magnetic powder content is high. This indicates that applying a magnetic field not only further optimizes the internal structure of the specimen but also makes the distribution of magnetic powder in the matrix more uniform, thereby more effectively reducing the formation of pores.

Table 2. CT and binarized image comparison of specimens after freeze-thaw cycles.

Magnetic field state	Magnetic powder content	CT image	Binarized image
No magnetic field applied	5%		
	10%		
	15%		
	20%		
	25%		
Magnetic field applied	5%		
	10%		
	15%		
	20%		
	25%		

Further analysis reveals that the magnetic powder content exerts a significant regulatory effect on the internal pore structure of the specimens. Regardless of whether an external magnetic field is applied during the specimen molding process, the internal porosity of the specimens shows a distinct downward trend as the magnetic powder content gradually increases. This phenomenon indicates that magnetic particles play a crucial densifying role in the slurry solidification process, their fine particle size enables them to effectively fill the pores. Meanwhile, the magnetic field has a notable optimizing effect on the pore structure. Under the condition of the same magnetic powder content, the porosity of specimens subjected to a magnetic field is generally lower than that of the control group without magnetic field application, and there is a clear difference between the two groups. This magnetic field effect is particularly prominent when the magnetic powder content is high, suggesting a synergistic enhancement effect between the magnetic field action and the magnetic powder content. The reduction in porosity directly diminishes the ability of water to penetrate into the interior of the specimens. When the specimens are exposed to freeze-thaw cycles, less internal water translates to reduced ice expansion pressure. This, in turn, lowers the risk of internal damage caused by frost heaving stress, thereby effectively improving the specimens' resistance to freeze-thaw cycles.

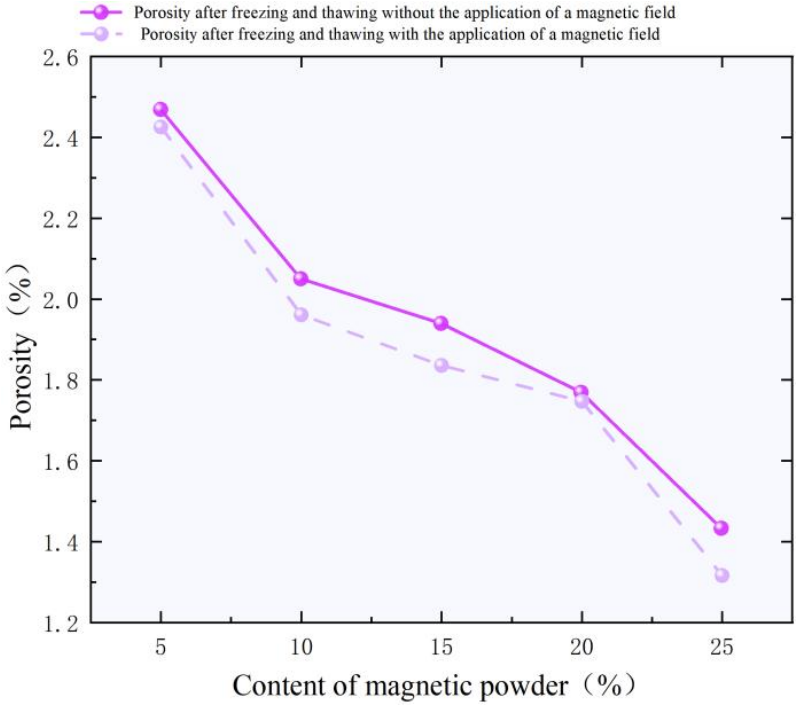


Figure 9. Porosity comparison of specimens after freeze-thaw cycles.

3.4. Magnetic chain analysis

Figure 10 clearly shows the distribution morphology of the magnetic slurry with a volume fraction of φ = 5% under different magnetic field conditions. When there is no applied magnetic field (B = 0Gs), the magnetic particles maintain a random distribution in the carrier liquid, with no obvious interaction between the particles, and the slurry system exhibits good flow characteristics at this time. As the applied magnetic field strength gradually increases to B = 100Gs, the microstructure of the magnetic slurry begins to change. Under the action of this magnetic field, the magnetic particles are attracted and start to show a tendency to approach and aggregate with each other. When the magnetic induction intensity is further increased to B =

1000Gs, the microstructure of the magnetic slurry undergoes a significant change. Under the action of a strong magnetic field, the magnetic particles are closely arranged along the direction of the magnetic field, forming a regular chain structure. Under this condition, there are roughly four different forms of particle chains in the magnetic slurry:

(1) Continuous chain: A complete particle chain that runs through the width direction of the image (or connects the front and back electrode plates).

(2) Branched chain: A particle chain that starts from one end of the image and terminates at a certain position in the image but does not run through the image (or a particle chain that originates from one electrode plate but does not connect to the other electrode plate).

(3) Isolated chain: A particle chain that is not connected to the electrode plates at both ends and floats in the carrier liquid.

(4) Bundle chain: A structure formed by the aggregation of multiple particle chains. Bundle chains are usually formed by the aggregation of continuous chains and isolated chains.

Due to the chain-like structure formed by the magnetic particles, the fluidity of the magnetic slurry decreases, and the resistance to shear deformation increases significantly.



(a) (b) (c)

Figure 10. Compressive strength loss after freeze-thaw cycles. **(a)** B=0 GS; **(b)** B=100 GS; **(c)** B=1000 GS.

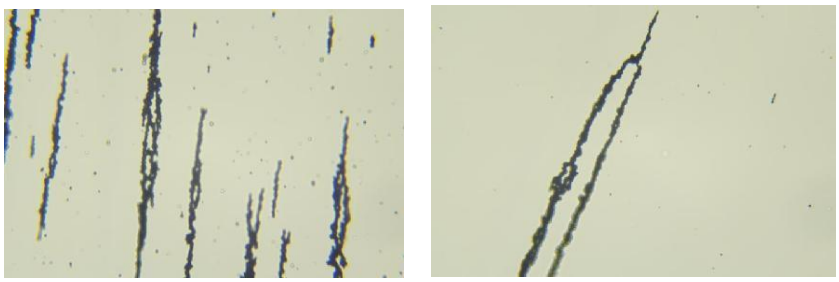


Figure 11. Magnetic particle chain distribution morphology (magnified 100 times).

3.5. The microscopic morphology after freeze-thaw action

As shown in the following figures, (a), (b), (c), (d), (e), and (f) respectively present the microscopic morphologies of samples with magnetic powder contents of 0%, 5%, 10%, 15%, 20%, and 25% after 25 freeze-thaw cycles. It can be clearly observed from the figures that the sample with 0% magnetic powder content has many internal cracks with large widths after 25 freeze-thaw cycles; the sample with 5% magnetic powder content suffers relatively severe internal damage, with long and wide cracks inside the structure, and the number of cracks is slightly less than that of the sample with 0% magnetic powder content; the internal

damage of the sample with 10% magnetic powder content is alleviated, with significantly reduced crack widths and a slight decrease in the number of cracks; when the magnetic powder content increases from 15%, the internal damage of the sample structure begins to be significantly mitigated. The number and width of cracks in the sample with 15% magnetic powder content are significantly less than those with 10% content, and the sample with 25% magnetic powder content has almost no cracks. This indicates that with the increase of magnetic powder content, the internal damage of the samples is reduced, the number and width of cracks decrease accordingly, and their ability to resist freeze-thaw cycles is stronger.

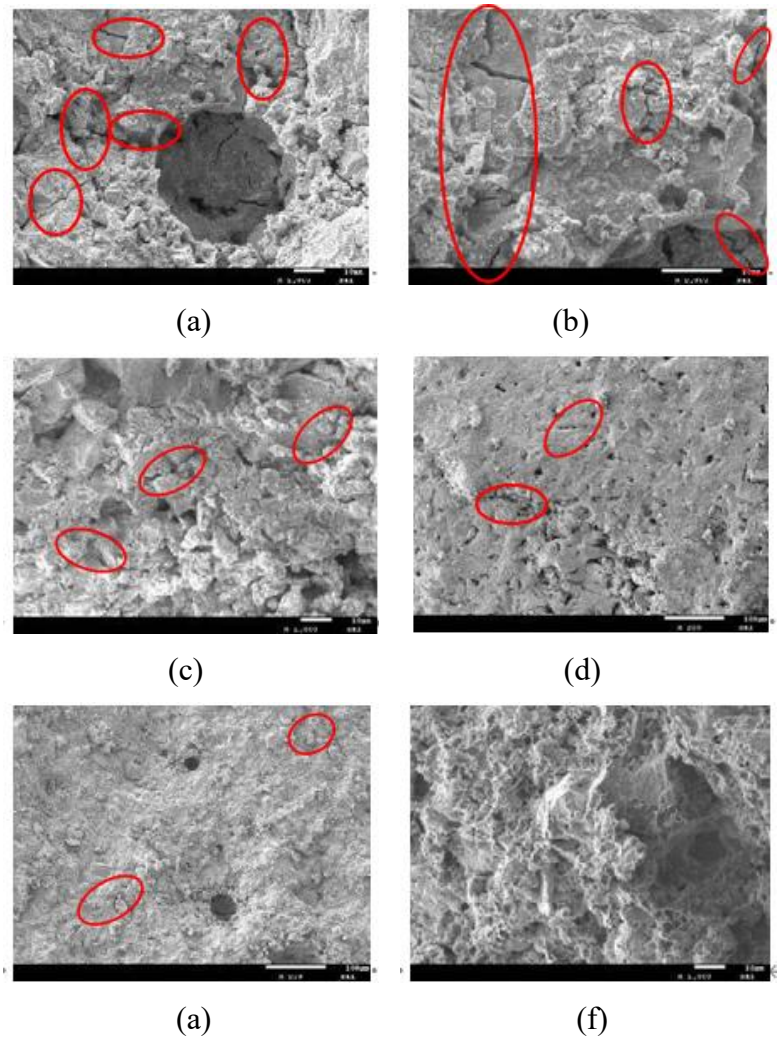


Figure 12. Microscopic morphology after 25 freeze-thaw cycles with different magnetic powder contents. **(a)** 0% magnetic powder content; **(b)** 5% magnetic powder content; **(c)** 10% magnetic powder content; **(d)** 15% magnetic powder content; **(e)** 20% magnetic powder content; **(f)** 25% magnetic powder content.

4. Conclusion

Under the same freeze-thaw cycle duration, as the mixing ratio of magnetic powder increases, the specimens exhibit more excellent damage resistance during the freeze-thaw cycles. The application of a magnetic field has an enhancing effect on the material's resistance to freeze-thaw cycles; compared with the specimens without a magnetic field applied, the magnetic slurry specimens with a magnetic field applied are less susceptible to damage caused by freeze-thaw cycles.

There is a positive correlation between the magnetic powder content and the compressive strength of the sample. As the magnetic powder content increases, the compressive strength of the magnetic slurry specimens also increases, and after undergoing freeze-thaw cycles, the loss of compressive strength of the specimens decreases. For specimens with the same magnetic powder content, the compressive strength of magnetic slurry specimens with a magnetic field applied is higher than that of those without a magnetic field, and the loss rate of compressive strength after freeze-thaw cycles is lower.

The content of magnetic powder has a significant impact on the internal pore structure of the sample. As the magnetic powder content increases, the internal porosity of the sample shows an obvious downward trend. The effect of magnetic field on improving porosity is very significant. Under the condition of the same magnetic powder content, the internal porosity of the sample with magnetic field applied is always lower than that of the sample without magnetic field applied. The reduction of porosity reduces the ability of moisture to penetrate into the interior of the sample.

From the microscopic morphology of the specimens after freeze-thaw cycles, it can be seen that the magnetic powder content can significantly improve the material's ability to resist damage from freeze-thaw cycles. The higher the magnetic powder content, the lighter the internal damage to the specimen structure, and the better the structural integrity is maintained.

There are four main particle chain morphologies in the magnetic slurry: through-chains, branched chains, isolated chains, and bundled chains. The existence of these chain-like structures reduces the fluidity of the magnetic slurry and increases the resistance to shear deformation. Although this study confirms the enhancing effect of magnetic chains on freeze-thaw resistance, establishing a quantitative model linking magnetic chain morphology to mechanical properties remains a challenge. Tackling this problem will be the focus of our future work.

Data availability statement

No supplementary or additional data were generated in this study.

Declaration of Generative AI and AI-assisted Technologies

During the preparation of this manuscript, the authors used generative AI tools only to improve language and readability. The authors take full responsibility for the content of the manuscript.

Authors' contribution

Conceptualization, Anlong Hu and Xinlong Yao; methodology, Anlong Hu and Yongsheng Ju; software, Jie Liu and Zhipeng Shang; validation, Yong Wei and Zhipeng Shang; formal analysis, Anlong Hu and Jie Liu; investigation, Yongsheng Ju and Yong Wei; resources, Xinlong Yao and Yongsheng Ju; data curation, Zhipeng Shang and Yong Wei; writing—original draft preparation, Anlong Hu; writing—review and editing, Jie Liu; visualization, Jie Liu and Zhipeng Shang; supervision, Anlong Hu; project administration, Anlong Hu and Yongsheng Ju; funding acquisition, Jie Liu. All authors have read and agreed to the published version of the manuscript.

Conflicts of interest

The authors declare that there are no potential conflicts of interest in this work, including but not limited to employment, consulting fees, research contracts, stock ownership, patent licenses, honoraria, advisory affiliations and other relevant situations.

References

[1] Rong X, Zheng S, Zhang Y, Zhang X, Dong L. Experimental study on the seismic behavior of RC shear walls after freeze-thaw damage. *Eng. Struct.* 2020, 206:110101.

[2] Asphaug SK, Kvande T, Time B, Peuhkuri RH, Kalamees T, *et al.* Moisture control strategies of habitable basements in cold climates. *Build. Environ.* 2020, 169:106572.

[3] Xu T, Zhou Z, Wang M, Zhu L, Tian Y, Han D. Damage mechanism of pier concrete subjected to combined compressive stress, freeze-thaw, and salt attacks in saline soil. *Constr. Build. Mater.* 2022, 324:126567.

[4] Wang J. Study on the evolution law of mechanical and moisture transport properties of air-entraining mortar before and after freezing and thawing and its micro-mechanism (In Chinese). Master's Thesis, Qingdao University of Technology, 2022.

[5] Pigeon M, Pleau R. *Durability of Concrete in Cold Climates,* 1st ed. London: Taylor & Francis, 1995. pp. 212.

[6] Zheng X, Wang Y, Zhang S, Xu F, Zhu X, *et al.* Research progress of the thermophysical and mechanical properties of concrete subjected to freeze-thaw cycles. *Constr. Build. Mater.* 2022, 330:127254.

[7] Wu W, Liu Y, Zhang Y, Huang J, Yan G*, et al.* Pore structure and mechanical properties of FRCC in the freeze-thaw environment: a review (In Chinese), *Mater. Rep.* 2023, 37(S1):23010108–12.

[8] Xu, Y, Fan Y. Effects of graphene oxide dispersion on salt-freezing resistance of concrete. *Adv. Mater. Sci. Eng.* 2020, 2020(1):4673739.

[9] Gollop RS, Taylor HFW. Microstructural and microanalytical studies of sulfate attack. I. Ordinary portland cement paste. *Cem. Concr. Res.* 1992, 22(6):1027–1038.

[10] Yu C, Sun W, Scrivener K. Mechanism of expansion of mortars immersed in sodium sulfate solutions. *Cem. Concr. Res.* 2013, 43: 105–111.

[11] Feng P, Garboczi E J, Miao C, Bullard JW. Microstructural origins of cement paste degradation by external sulfate attack. *Constr. Build. Mater.* 2015, 96: 391–403.

[12] Zhang M, Jiang M, Chen J. Variation of flexural strength of cement mortar attacked by sulfate ions. *Eng. Fract. Mech.* 2008, 75(17): 4948–4957.

[13] Sun R, Lu W, Ma C, Tawfek AM, Guan Y, *et al.* Effect of crack width and wet-dry cycles on the chloride penetration resistance of engineered cementitious composite (ECC). *Constr. Build. Mater.* 2022, 352:129030.

[14] Liu J, Zhang K, Li Z, Liu Z, Mao K. Research on the pore size distribution and durability improvement mechanism of magnetic slurry. *Sci. Rep.* 2025, 15(1):37613.

[15] Hu F, Wu H, Jiao D. Effect of magneto-rheological response on early hydration and microstructure of cement paste. *Constr. Build. Mater.* 2025,474:141161.

[16] Bai R, Liu S, Yin L, Yan C, Zhou J, *et al.* Freeze-thaw damage assessment of engineered cementitious composites using the electrochemical impedance spectroscopy method. *Mater. Des.* 2023, 230:111965.